Research article

Journal of RAMAN SPECTROSCOPY

Received: 24 December 2013 Revised: 14 April 2014 Accepted: 9 May 2014 Published online in Wiley Online Library

(wileyonlinelibrary.com) DOI 10.1002/jrs.4518

The influence of UV–Vis radiation, and oscillations of temperature and relative humidity, on malachite alteration in the presence of different organic binders and varnishes†

Tanja Špec,[a]* Klara Retko,[a] Polonca Ropret,[a,b] Anton Meden[c] and Janez Bernard[d]

The presented study describes the deterioration of a traditional pigment, malachite—[$Cu_2(CO_3)(OH)_2$] in different binders, as a consequence of environmental effects acting on paint layers which were prepared according to traditional Baroque recipes. Malachite has often been reported to be very permanent in all binding media; however, investigations of aged and non-aged paint layers by means of Raman microscopy have shown instability of the carbonate part of the molecule, especially when malachite is present in an egg yolk medium. Decomposition of the pigment and the formation of degradation products such as copper oxide (tenorite—CuO) were observed. The possible formation of another copper oxide, paramelaconite—Cu_4O_3 was also taken into consideration. In order to obtain additional information on the degradation processes which affect malachite paint layers, supporting analytical methods, such as scanning electron microscopy and X-ray diffraction, were used.

Keywords: malachite; accelerated ageing; Raman microscopy; copper oxides

Introduction

The precise characterization of materials which are present in works of art, and examination of their degradation processes, has a great impact on the understanding of the different degradation processes which affect pigments, binders, protective layers, as well as their possible interactions. Such research work can make an important contribution to the development of safer, long-term restoration and conservation procedures. The degradation processes of cultural heritage materials are, due to diversity of their causes, complex. For example, they can be a consequence of inappropriate climate conditions which may accelerate the decomposition of organic or inorganic materials, as well as interactions between the different components, or they can be a result of the tendency to ageing according to the structure of the material itself. The understanding of such phenomena can be further complicated by the heterogeneity of the used materials and their various interactions.

Materials used in paintings can be investigated using numerous different analytical approaches, such as Raman microscopy (RM),[1–4] scanning electron microscopy (SEM),[5,6] Fourier Transform infrared spectroscopy (FT-IR),[7,8] X-ray fluorescence (XRF),[9,10] X-ray diffraction (XRD),[11,12] synchrotron radiation based X-ray techniques (μ-XANES, μ-EXFAS, μ-XRF, μ-FT-IR, μ-XRD, μ-XRF…),[13–18] chromatographic,[19,20] immunological techniques,[21,22] etc. Among other analytical methods, RM is frequently used in the field of the cultural heritage since it is, in fact, an effective tool for the detection of various different inorganic components, such as pigments and minerals,[2,23] as well as corrosion products.[24–26] Thus, RM can be used to investigate mural paintings,[12,27] easel paintings,[28,29] textiles,[30,31] ceramics and glass,[32,33] etc. Moreover, in the case of paintings that have several layers, the technique can provide vibrational information about layers of interest, when analysing the cross section of a sample. It can also provide precise knowledge about which materials have been subjected to degradation according to their location and the composition of the layer. Its non-destructive character, high sensitivity and micrometric spatial resolution are the benefits of its application for the study of degradation processes. Due to the variety of materials used in traditional paintings, the systematic study of materials characterization and

* *Correspondence to: Tanja Špec, Institute for the Protection of Cultural Heritage of Slovenia, Research Institute, Conservation Centre, Poljanska 40, SI-1000 Ljubljana, Slovenia.*
E-mail: tanja.spec@zvkds.si

† *This article is part of the special issue of the Journal of Raman Spectroscopy entitled "Raman in Art and Archaeology 2013" edited by Polonca Ropret and Juan Manuel Madariaga.*

a *Institute for the Protection of Cultural Heritage of Slovenia, Research Institute, Conservation Centre, Poljanska 40, SI-1000 Ljubljana, Slovenia*

b *Museum Conservation Institute, Smithsonian Institution, 4210 Silver Hill Rd., Suitland, MD, 20746 USA*

c *University of Ljubljana, Faculty of Chemistry and Chemical Technology, Aškerčeva 5, SI-1000 Ljubljana, Slovenia*

d *Slovenian National Building and Civil Engineering Institute, Dimičeva 12, SI-1000 Ljubljana, Slovenia*

assessment of the degradation processes require careful decisions with respect to the applied analytical method.

To acquire a better understanding of pigments, their interactions with accompanying materials, determination of their degradation products and specifications with respect to further degradation processes, many studies have been carried out on traditional pigments, such as lead white,[34–36] vermilion,[37–39] azurite,[40,41] malachite,[42–45] natural ultramarine,[46] smalt,[47] prussian blue,[48] lead tin yellow (type I),[36,49–51] red lead,[36,52] verdigris,[53] lapis lazuli[54] and madder lakes.[55,56]

Malachite, the basic copper carbonate [$Cu_2(CO_3)(OH)_2$], is historically one of the oldest green pigments, and has been used to a great extent in different works of art from Antiquity until the late 1800s.[57] It has often been reported to be permanent and unaffected by strong light or alkalis.[12] On the other hand, malachite and other copper pigments are sensitive to environmental pollutants, where transformation into copper chlorides (atacamite, paratacamite) or sulphates (brochantite, prosnjakite and langite) has been reported by several authors.[44,58–60] Moreover, when exposed to biochemical activity, such as lichens, fungi or bacteria, which are strong producers of oxalic acid, transformation into copper oxalates may occur.[42,43] In works of art, decomposition of copper pigments into the copper oxide tenorite is more characteristic for another carbonate of copper, azurite [$Cu_3(CO_3)_2(OH)_2$], which is likely to decompose in the presence of alkalis and heat.[61] However, due to its similar structure, the formation of tenorite needs to be taken into account also in the case of malachite-containing paint layers.

The aim of this work was to study the decomposition of malachite paint layers, and the formation of degradation products in easel paintings, where different combinations of binders and varnishes have been used. Special attention was paid to the formation of degradation products caused by UV–Vis radiation, exposure to humidity and temperature oscillations.

Experimental

Materials

The malachite pigment used in this study was purchased from Kremer Chemicals as a Malachite natural standard (Kremer pigments, 10300). Sun-bleached linseed oil was purchased from Lefrance & Bourgeois. Gummi Mastic was purchased from Kremer Chemicals Nr. 60050 and mixed with Fir Turpentine, purchased from Kremer Chemicals Nr. 70010. (The ratio between the Gumi Mastic and the Fir Turpentine was 1:3).

Preparation of the model paintings

Easel (model) paintings containing malachite paint layers were prepared according to traditional Baroque recipes. The canvas was stretched across a wooden sub-frame and treated with a hot rabbit glue solution. Subsequently, white Gesso ground was applied. After it had dried, the surface was polished with sand papers. The Gesso application procedure was repeated three times.

Four different binders were used as binding media: non-fatty egg tempera, fatty egg tempera (egg tempera mixed with linseed oil), linseed oil and linseed oil mixed with mastic. In order to prepare the egg tempera, one egg yolk was mixed with the same volume of water and a drop of apple cider vinegar was added. For the remaining binders, commercially available linseed oil and mastic were used. The paint was prepared by grinding the pigment (malachite) together with the medium. After this, the prepared malachite paint was applied to the Gesso ground.

As finishing protective layers, egg white and mastics were applied to the malachite paint layers. In order to prepare the egg white, it was separated from the yolk and beaten until foam was formed. The egg white was then left to stand in a fridge for one night, and the foam was separated from the liquid part. Two grams of sugar per egg was added to the liquid part of the egg white.[62,63]

Environmental exposure

The prepared easel (model) paintings were exposed to accelerated artificial ageing in climatic chambers with a well-defined and controlled temperature and relative humidity, as well as light conditions.

For the simulation of UV–Vis radiation, a metal halide lamp (with an irradiance of 100 W/m^2) was used. It was equipped with window glass filters, so that good simulation of sun light was achieved. Thirty days of light exposure was followed by another 30-day exposure in the climatic chamber, with oscillations of the temperature and relative humidity (from 0 °C to 50 °C, and from 20% to 90%, respectively).

Sample preparation

Micro samples were collected from the malachite paint layers of the model painting, embedded in a polyester casting resin, and then ground and polished. One sample was collected from a green paint layer of the easel painting entitled '*Madonna of the Rosary*' (17^{th} century, unknown author), which was selected for the case study. The cross sections of the micro samples were then examined by means of an Olympus BX 60 microscope, which was connected to a JVC 3-CCD video camera using visible light. Further characterization of the cross-sections of the samples was performed by making use of RM, SEM/energy dispersive spectrometry (EDS) and XRD.

Methods

RM

The Raman spectra of paint layers were recorded using a 785-nm laser excitation line with a Horiba Jobin Yvon LabRAM HR800 Raman spectrometer coupled to an Olympus BXFM optical microscope. The spectra were recorded using a 100× objective lens and a 600 grooves/mm grating, which gave a spectral resolution of 0.83 cm^{-1}/pixel. The power at the samples was set to between 0.4 and 26.9 mW, using neutral density filters. A multi-channel, air-cooled CCD detector was used, with integration times of between 20 and 50 s, and the spectral range was set to between 50 and 4000 cm^{-1}. The wave number calibration was performed using a silicon wafer. For each non-aged malachite paint layer, five spectra were recorded, whereas in the case of the aged layers, 10–15 spectra were recorded. The spectra were baseline corrected and normalized. The average spectra were calculated using the OPUS 7.0 data collection software package (Bruker, Germany).

SEM/EDS

The microstructures of the paint layers in the cross sections of the samples were observed by means of a scanning electron microscope—SEM (Jeol 5500 LV, Japan), using an acceleration voltage

Journal of RAMAN SPECTROSCOPY

of 20 kV. The elemental chemical compositions of the selected sample surfaces were determined by energy dispersive spectroscopy, which was controlled by INCA software (Oxford Instruments, UK). For point analysis, the spectra acquisition times were 60 s. SEM examinations of the samples were performed in the low-vacuum mode in order to avoid the need for sputtering, and thus preserve the samples for further investigations.

XRD

Diffraction patterns of the samples were recorded by using a PANalytical X'Pert Pro MPD diffractometer (PANalytical, Netherlands) with CuKα radiation (1.541874 Å) in the 2-θ range from 10 to 80° in steps of 0.039°, and an integration time of 100 s per step (the full range of the PIXcel detector, covering 3.347° 2θ was used). The patterns were collected during heating of the samples, which was performed in an Anton Paar HTK-1200 oven-type chamber which was mounted on the diffractometer. The heat conditioning consisted of heating from 25 °C to 500 °C, followed by cooling down to room temperature. In the temperature range from 250 °C to 400 °C, the patterns were recorded with increments of 10 °C (the heating rate between individual data collections was 10 °C/min), whereas at other temperatures a 50 °C increment was used. In order to improve the signal-to-noise ratio for the phase analysis of the decomposition products of the specimens after they had been cooled to room temperature, a series of diffraction patterns (260) were collected and merged (resulting in an effective integration time of 26.000 s per step). The diffraction patterns were processed using X'Pert HighScore Plus version 2.2d (PANalytical, Netherlands) software.

Results and discusion

RM results of the aged and non-aged malachite paint layers

Raman bands of malachite were determined in the spectra of all the control samples (Fig. 1), where the bands were in good agreement with the data in the literature[2] and were found at: 153, 166, 179, 218, 269, 354, 431, 512, 531, 596, 717, 750, 1058, 1096, 1369 and 1492 cm^{-1}. The analyses carried out on the aged samples of malachite paint layers not protected by varnish layers (egg white or mastic) showed the most pronounced differences when egg yolk was present as a binder. When comparing the Raman spectra of malachite paint layers prepared in unfatty (egg yolk) and fatty egg (egg yolk, linseed oil) tempera, a decrease in the relative intensities of the bands assigned as carbonate symmetric (ν_1) at 1059 cm^{-1} and carbonate asymmetric (ν_3) at 1495 cm^{-1}—stretching vibrations was observed (Fig. 1 (a),(b)).[64] These results are corroborated by the results of calculations of the ratio of the relative intensities of the asymmetric (ν_3) and symmetric (ν_1) stretching vibrations, which is 1.5 in the case of the non-aged samples, and decreased to 0.7 in the case of the corresponding aged samples. (Table 1,a)). For the malachite paint layer where oil was added to the binding media (fatty egg yolk tempera and linseed oil), some differences can be seen in the ratio ν_3/ν_1, but they are less prominent. (Table 1,(b, c)). According to the Raman spectra of the analysed samples prepared with malachite, linseed oil and mastic (Fig. 1(d)) and the calculated ratio ν_3/ν_1 (Table 1, d)), it can be concluded that these colour layers are the most stable.

The Raman spectra of the malachite colour layers, coated with finishing protective layers such as mastic and egg white, are shown in Fig. 2. Degradation of the malachite layers, which was evident from the decrease in the relative intensities of the bands

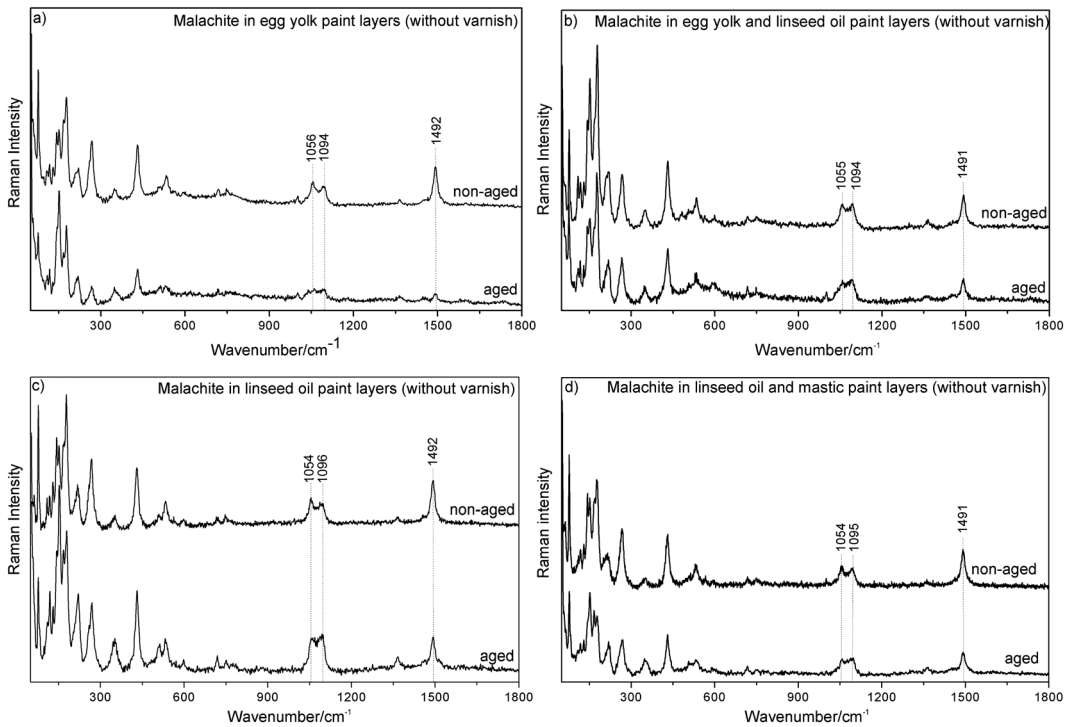

Figure 1. Comparison of the Raman spectra of the malachite paint layer prepared (a) in egg yolk, before and after ageing, (b) in egg yolk and linseed oil, before and after ageing, (c) in linseed oil, before and after ageing and (d) in linseed oil and mastic, before and after ageing.

Table 1. The ratios between the relative intensities of carbonate asymmetric (v_3) and symmetric (v_1) stretching vibrations in malachite paint layers prepared in different binders without varnishes

	a)		b)		c)		d)	
	Unfatty egg tempera		Fatty egg tempera		Linseed oil		Linseed oil and mastic	
Binder	Non-aged	Aged	Non-aged	Aged	Non-aged	Aged	Non-aged	Aged
Intensity ratio v_3/v_1	**1.5**	**0.7**	**1.3**	**0.9**	**1.4**	**0.9**	**1.7**	**1.3**

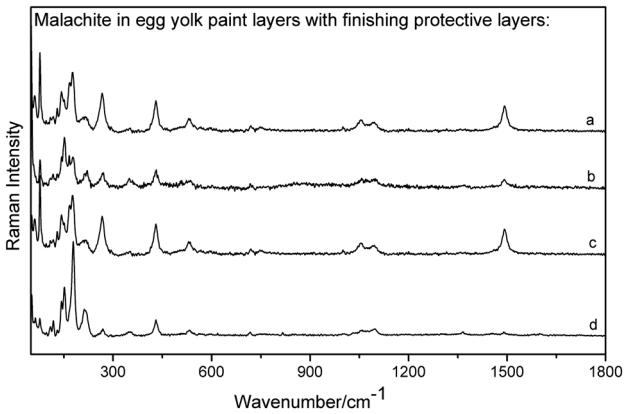

Figure 2. Comparison of the Raman spectra of the malachite paint layers prepared in egg yolk coated with (a) egg white and mastic (non-aged), (b) egg white and mastic (aged), (c) egg white (non aged) and (d) egg white (aged).

located at 1059 and 1495 cm^{-1} (v_1 CO_3^{2-}, v_3 CO_3^{2-}) (Fig. 2(b),(d)), was observed only in the malachite colour layers that had been prepared with an egg yolk. The values of the calculated ratio v_3/v_1 are shown in Table 2. According to these results, malachite paint layers prepared with an egg yolk and protected with both varnishes are more stable than those protected with only one finishing protective layer of egg white. For the remaining colour layers protected with a finishing protective coating, no changes in the relative intensities were observed (these spectra are not shown).

Small variations were observed in the symmetric and asymmetric stretching vibrations of the carbonate group band positions when linseed oil was added to the binder. From 1056 cm^{-1} in egg yolk to 1055 cm^{-1} in the mixture of egg yolk and linseed oil, and to 1054 cm^{-1} when only oil were used as a binder. On the other hand, a shift to a higher wavenumber was observed in the case of the asymmetric stretching vibrations of the carbonate group. From 1490 cm^{-1} in egg yolk to 1491 cm^{-1} in the mixture of egg yolk and linseed oil, and 1492 cm^{-1} when only oil were used as a binder. These results suggest instability of the malachite carbonate group in paint layers when egg yolk and linseed oil are used as binders. Furthermore, in the case of egg yolk, the protection achieved by the application of varnish layers was not enough to prevent deterioration.

Utilizing RM, characterization of pigments was also performed along the cross section of a sample removed from a green layer of the Baroque painting entitled '*Madonna of the Rosary*' (Fig. 3(a) and (b)). Investigation of particles, marked as MDR_1 and MDR_2 (Fig. 3(c)) showed Raman bands at ~ 153, 177, 217, 268, 353, 433 and 1098 cm^{-1} for MDR1 and at ~ 153, 177, 217, 268, 353, 433, 1098 and 1495 cm^{-1} for MDR_2 (Fig. 3(d)), which was sufficient for a positive identification of malachite. However, a decrease in the relative intensity of the bands that are significant for carbonate symmetric (v_1) at 1059 cm^{-1} and asymmetric (v_3) at 1369 and 1495 cm^{-1} stretching vibrations was noticed. Similar to the previously described results for the malachite model paint layers, instability of the malachite carbonate group was also noticed for this selected case study.

Micro-Raman analyses of dark particles on a green malachite paint layer

Apart from the green particles of malachite, black particles were also seen in the cross sections of all of the samples. Nevertheless, a much higher proportion of the latter was observed in the aged samples (Fig. 4(a)). The exposure of malachite paint layers to artificial ageing resulted in transformation of the pigment, and a colour change of malachite particles as a consequence of the degradation process. The Raman bands of the analysed black particles, at 296, 346 and 608 cm^{-1} (Fig. 4(b)) indicate the presence of a copper oxide: tenorite (CuO). However, differences in the spectra between the reference material and the sample can be seen, especially in the relative intensities of the bands at 296

Table 2. The ratios between the relative intensities of carbonate asymmetric (v_3) and symmetric (v_1) stretching vibrations in malachite paint layers prepared in egg yolk and: a) protected only by egg white; b) protected by egg white and a second layer of mastic

Varnishes	a)		b)	
	Non-aged	Aged	Non-aged	Aged
Intensity ratio v_3/v_1	**1.8**	**0.8**	**1.4**	**0.8**

Journal of RAMAN SPECTROSCOPY

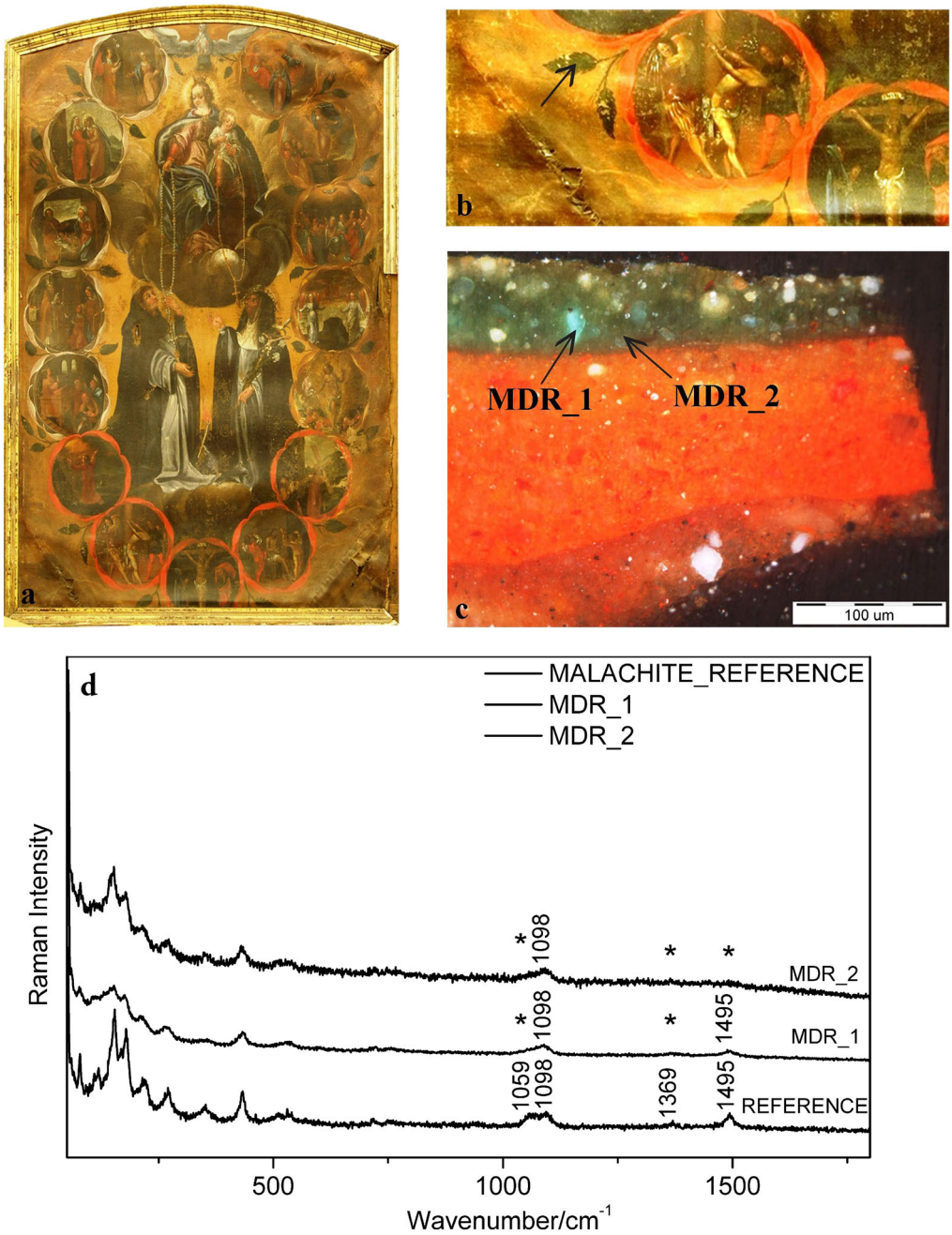

Figure 3. (a) Photo of the picture 'Madonna of the Rosary', by an unknown Slovenian author (cca. 17th century). (b) Detail of the sampling area (green leaf). (c) Photomicrograph of the polished cross section of the removed sample. (d) Comparison of the Raman spectra of the reference material of the green particles (MDR_ 1 and MDR_2).

and 603 cm^{-1}. The presence of an another copper oxide, paramelaconite Cu_4O_3, was suggested, supported by the presence of an additional very weak band at 320 cm^{-1} and a shoulder at 541 cm^{-1}, which can be assigned to its E_g and A_{1g} modes, respectively.[65] In this oxide, copper is present in both oxidation states, Cu(I) and Cu(II). Despite the close relation of the two structures (Cu_4O_3 can be described as a CuO crystal without a monoclinic distortion, where one-quarter of the oxygen atoms has been removed), RM proved to be a good method for distinguishing between tenorite and paramelaconite.[65] However, in the actual case, the Raman bands, which could belong to paramelaconite, were too weak for a positive identification to be made. In order to gain further information about the black particles in the malachite paint layers, two supporting analytical techniques, i.e. SEM/EDS and XRD, were employed.

SEM/EDS analyses of the dark particles

A SEM/BE (back-scattered electron) micrograph of the polished surface of one of the aged specimens of paint layers containing

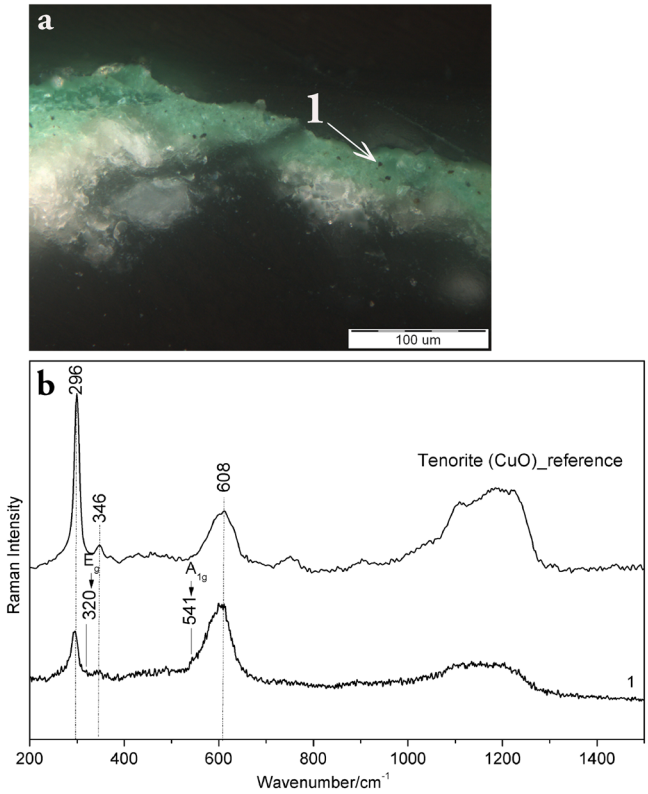

Figure 4. (a) Photomicrograph of the polished cross section of a malachite paint layer, prepared in egg yolk with linseed oil and aged. (b) Comparison of the Raman spectra of tenorite (reference material) and the dark particles on the malachite paint layer (Spectrum of particle 1, see Fig. 4(a)).

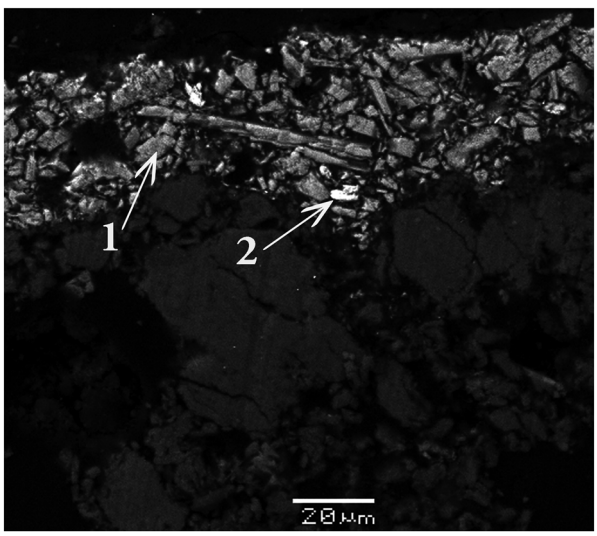

Figure 5. The SEM/BE image of the polished cross section of the aged sample of the malachite paint. Layer 1 shows the elemental EDS analysis of the green layer, whereas 2 shows the EDS analysis of a dark particle in the green layer.

malachite is presented in Fig. 5. The top paint layer, with bright pigment particles, can be easily distinguished from the dark ground layer. EDS analysis revealed the elemental composition of the pigment (Table 3). Malachite particles contain a considerable amount of copper (1.3% to 2.5%). Note that the pigment particles are quite heterogeneous, so that precise EDS analysis could not be performed. A small number of dark particles were found on the non-aged samples, these particles containing higher amounts of copper. However, the proportion of dark particles was higher in the case of the aged samples, where the concentration of copper in the dark pigment particles, found in the malachite paint layer (Fig. 5, the particle denoted as 2), was much higher than could be expected for malachite (Table 3). According to these results, the formation of dark particles on malachite paint layers is caused by ageing processes.

XRD analysis

XRD powder patterns were obtained during controlled heating of the raw malachite powder from 25 °C to 500 °C, followed by cooling to room temperature. At 25 °C, the powder primarily consists of monoclinic malachite (PDF card 010-72-8421) and some traces of a secondary phase, which can be detected by a peak at a 2θ angle of around 20°, which does not belong to malachite. It is assumed that the presence of a secondary phase is a consequence of impurities, presented in the natural sourced malachite (Fig. 6).

The malachite started to decompose at approximately 300 °C, where its diffraction peak intensities started to decrease. At 400 °C, it decomposed completely into monoclinic tenorite (PDF card 010-70-6831), whereas the impurities were not affected by temperature and were still present in the specimen. On the basis of the presented XRD analysis, the occurrence of paramelaconite as a product of the thermal decomposition of malachite could not be confirmed. Despite a quite significant overlap of the diffraction peaks of paramelaconite with those of tenorite, there is a relatively strong (relative intensity of 17%, compared to the highest peak) non-overlapping peak of paramelaconite at a 2θ angle of about 40° (PDF card 040-08-4362). According to our experience with similar samples, the detection limit of paramelaconite in a mixture with tenorite could, in a routinely measured pattern, such as the one that is labelled 'a' in the inset shown in Fig. 6, be up to 2 or 3% (the noise can be clearly seen).

In order to improve the detection limit for the possible presence of paramelaconite in the malachite decomposition product (tenorite), a series of 260 diffraction patterns (a week-end run) of the specimen cooled to 25 °C were collected and merged. The inset in Fig. 6 shows the 2θ range from 40° to 50° of (a) the specimen heated to 400 °C, and (b) the merged pattern of the cooled specimen. It can be seen that the noise in (b) was significantly less, and it was estimated that the detection limit of paramelaconite was, in this case, less than 0.5%. However, the (1 2 3) peak of tetragonal paramelaconite at 2θ = 44° was not detected in the merged pattern. It can be concluded that, most probably, paramelaconite is not formed at all during thermal decomposition of the specimen, when the latter is heated to 400 °C. If it is formed, then its quantity in the final cooled specimen is very low (definitely less than 0.5%). It may, however, form as a transition product in somewhat higher quantities (up to 3%) without being detected by XRD analysis.

Journal of RAMAN SPECTROSCOPY

Table 3. Elemental EDS analysis of the malachite paint layers

Material/%	C	Si	S	Ca	Cu	O
Malachite paint layer						
Green particle in the non-aged sample	26.32	0.04	0.42	0.57	1.30	71.35
Dark particle in the non-aged sample	21.10				18.14	60.77
1: Green particle in the aged sample	24.91	0.14	1.27	0.16	2.45	69.62
2: Dark particle in the aged sample	18.92			0.28	24.21	56.60

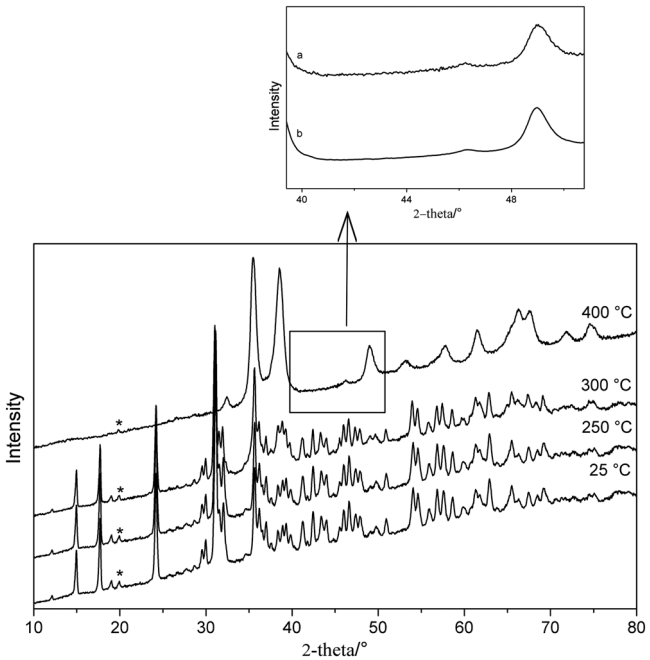

Figure 6. XRD powder patterns of malachite powder obtained during heating at 25 °C, 250 °C, 300 °C and 400 °C. The diffraction peak denoted by (*) corresponds to an impurity. The inset corresponds to the pattern of a specimen heated to 400 °C (a), and the merged pattern of a cooled specimen (b). 164 × 161 mm (600 × 600 DPI).

Conclusions

An extended study on the degradation of malachite paint layers was carried out, by preparing easel (model) paintings and exposing them to different environmental parameters (UV–Vis radiation, temperature and humidity oscillations). When RM was applied to aged and non-aged samples, a decrease in the intensity of the bands assigned to symmetric and asymmetric carbonate stretching (~1496, 1369, 1098 and 1059 cm^{-1}) was observed. This decrease was much more pronounced in cases when egg tempera was used as a binder. Even when the finishing protective layers, such as egg white and mastic, were applied, the paint layers of malachite prepared in egg tempera showed a lower level of stability than when prepared in linseed oil. Investigation of green paint layers was also performed on the painting entitled '*Madonna of the Rosary*', which has been dated to the 17th century and is by an unknown Slovenian artist. RM analyses showed similar results with regard to the decomposition of malachite (a decrease in the intensity of the malachite characteristic bands at ~ 1496, 1369, 1098 and 1059 cm^{-1}), as in the case of the model paints. This means that malachite-containing paints are prone to degradation also when subjected, over centuries, to real life conditions.

As well as green particles of malachite, black particles, too, were observed in cross sections of all the samples, although a higher proportion of them was detected in the case of the aged samples. Additionally, the results of SEM/EDS showed an increased relative amount of copper in the dark particles in comparison with the green ones. Using RM, the presence of the copper oxide tenorite was confirmed, and the presence of another oxide—paramelaconite was suspected.

In order to confirm the presence of paramalaconite as a decomposition product of malachite, *in-situ* XRD analyses were performed during thermal decomposition of the malachite samples. Paramelaconite was not detected, either due to its very small concentration, but more likely it is not formed during the thermal decomposition of malachite in air. This is because, in the ageing process described in the experimental part, the specimen is exposed to conditions which differ significantly from those in the case of heating, so that it is quite possible that the decomposition path of the malachite is different in these two cases.

For a more complete investigation, some other analytical techniques should be used in order to overcome the above-mentioned ambiguities. The detection of paramelaconite, where copper is present in two different oxidation states (I, II), would be possible if synchrotron-based spectroscopic methods, such as μ-XANES, were used, in which point analyses of the sample's cross section can be performed, and distinctions made between the different oxidation states of the metal. In their further research, the authors intend to expand this study by making use of this method.

Acknowledgements

The financial support of the Slovenian Research Agency (grant L6-4217) is much appreciated. This paper is also a result of doctoral research, in part financed by the European Union, European Social Fund and the Republic of Slovenia, Ministry for Education, Science and Sport within the framework of the Operational programme for human resources development for the period 2007–2013 (n° 3330-13-500221).

The authors would also like to thank Barbka Gosar Hirci, academic painter, Head of the Easel Paintings Department (Institute for the Protection of Cultural Heritage of Slovenia, Conservation Centre, Restoration Centre) for help with the preparation of the model paintings.

References

[1] P. Vandenabeele, H. G. M. Edwards, L. Moens, *Chem. Rev.* **2007**, *107*, 675.
[2] I. M. Bell, R. J. H. Clark, P. J. Gibbs, *Spectrochim. Acta A Mol. Biomol. Spectrosc.* **1997**, *53*, 2159.
[3] L. Burgio, R. J. H. Clark, *Spectrochim. Acta A Mol. Biomol. Spectrosc.* **2001**, *57*, 1491.

[4] M. Castillejo, M. Martín, D. Silva, T. Stratoudaki, D. Anglos, L. Burgio, R. J. H. Clark, *J. Mol. Struct.* **2000**, 550–551, *191*.
[5] M. Irazola, M. Olivares, K. Castro, M. Maguregui, I. Martínez-Arkarazo, J. M. Madariaga, *J. Raman Spectrosc.* **2012**, *43*, 1676.
[6] A. Sever-Škapin, P. Ropret, *Adv. Imag. Electron Phys.* **2010**, *163*, 141.
[7] S. Prati, E. Joseph, G. Sciutto, R. Mazzeo, *Acc. Chem. Res.* **2010**, *43*, 792.
[8] Z. Kaszowska, K. Malek, M. Pańczyk, A. Mikołajska, *Vib. Spectrosc*, **2013**, *65*, 1.
[9] B. Wehling, P. Vandenabeele, L. Moens, R. Klockenkämper, A. von Bohlen, G. V. Hooydonk, M. de Reu, *Microchim. Acta*, **1999**, *130*, 253.
[10] L. Burgio, R. J. H. Clark, R. R. Hark, *Proc. Natl. Acad. Sci. U. S. A.*, **2010**, *107*, 5726.
[11] R. J. H. Clark, M. L. Curri, *J. Mol. Struct.***1998**, *440*, 105.
[12] S. Švarcová, D. Hradil, J. Hradilová, E. Kočí, P. Bezdička, *Anal. Bioanal. Chem.* **2009**, *395*, 2037.
[13] L. Bertrand, M. Cotte, M. Stampanoni, M. Thoury, F. Marone, S. Schöder, *Phys. Rep.* **2012**, *519*, 51.
[14] G. Van der Snickt, K. Janssens, J. Dik, W. De Nolf, F. Vanmeert, J. Jaroszewicz, M. Cotte, G. Falkenberg, L. Van der Loeff, *Anal. Chem.* **2012**, *84*, 10221.
[15] L. Monico, G. Van der Snickt, K. Janssens, W. De Nolf, C. Miliani, J. Verbeeck, H. Tian, H. Tan, J. Dik, M. Radepont, M. Cotte, *Anal. Chem.* **2011**, *83*, 1214.
[16] L. Monico, G. Van der Snickt, K. Janssens, W. De Nolf, C. Miliani, J. Dik, M. Radepont, E. Hendriks, M. Geldof, M. Cotte, *Anal. Chem.* **2011**, *83*, 1224.
[17] L. Monico, K. Janssens, C. Miliani, B. G. Brunetti, M. Vagnini, F. Vanmeert, G. Falkenberg, A. Abakumov, Y. Lu, H. Tian, J. Verbeeck, M. Radepont, M. Cotte, E. Hendriks, M. Geldof, L. van der Loeff, J. Salvant, M. Menu, *Anal. Chem.* **2013**, *85*, 851.
[18] L. Monico, K. Janssens, C. Miliani, G. Van der Snickt, B. G. Brunetti, M. Cestelli Guidi, M. Radepont, M. Cotte, *Anal. Chem.* **2013**, *85*, 860.
[19] J. Kolar, J. Malešič, D. Kočar, M. Strlič, G. De Bruin, D. Koleša *Polym. Degrad. Stabil.* **2012**, *97*, 2212.
[20] T. Reeves, R. S. Popelka-Filcoff, C. E. Lenehan, *Anal. Chim. Acta*, **2013**, *803*, 194.
[21] M. Palmieri, M. Vagnini, L. Pitzurra, P. Rocchi, B. G. Brunetti, A. Sgamellotti, L. Cartechini, *Anal. Bioanal. Chem.* **2011**, *399*, 3011.
[22] G. Sciutto, L. S. Dolci, M. Guardigli, M. Zangheri, S. Prati, R. Mazzeo, A. Roda, *Anal. Bioanal. Chem.* **2013**, *405*, 933.
[23] F. Froment, A. Tournié, P. Colomban, *J. Raman Spectrosc.* **2008**, *39*, 560.
[24] G. Bertolotti, D. Bersani, P. P. Lottici, M. Alesiani, T. Malcherek, J. Schlüter, *Anal. Bioanal. Chem.* **2012**, *402*, 1451.
[25] P. Ropret, T. Kosec, *J. Raman Spectrosc.* **2012**, *43*, 1578.
[26] T. Kosec, P. Ropret, A. Legat, *J. Raman Spectrosc.* **2012**, *43*, 1587.
[27] G. E. De Benedetto, D. Fico, E. Margapoti, A. Pennetta, A. Cassiano, B. Minerva, *J. Raman Spectrosc.* **2013**, *44*, 899.
[28] E. Cazzanelli, E. Platania, G. De Santo, A. Fasanella, M. Castriota *J. Raman Spectrosc.* **2012**, *43*, 1694.
[29] M. Ortega-Avilés, P. Vandenabeele, D. Tenorio, G. Murillo, M. Jiménez-Reyes, N. Gutiérrez, *Anal. Chim. Acta*, **2005**, *550*, 164.
[30] G. Fanti, P. Baraldi, R. Basso, A. Tinti, *Vib. Spectrosc.* **2013**, *67*, 61.
[31] D. Gong, H. Yang, *Polym. Degrad. Stabil.* **2013**, *98*, 1780.
[32] P. Colomban, *Appl. Phys. A.* **2004**, *79*, 167.
[33] D. Barilaro, G. Barone, V. Crupi, M. G. Donato, D. Majolino, G. Messina, R. Ponterio, *J. Mol. Struct.* **2005**, *744-747*, 827.
[34] N. S. Cohen, M. Odlyha, R. Campana, G. M. Foster, *Thermochim. Acta*, **2000**, *365*, 45.
[35] E. Kotulanová, P. Bezdička, D. Hradil, J. Hradilová, S. Švarcová, T. Grygar, *J. Cult. Herit.* **2009**, *10*, 367.
[36] L. Burgio, R. J. H. Clark, S. Firth, *Analyst*, **2001**, *126*, 222.
[37] M. Cotte, J. Susini, N. Metrich, A. Moscato, C. Gratziu, A. Bertagnini, M. Pagano, *Anal. Chem.* **2006**, *78*, 7484.
[38] K. Keune, J. J. Boon, *Anal. Chem.* **2005**, *77*, 4742.
[39] J. K. McCormack, *Miner. Deposita*, **2000**, *35*, 796.
[40] M. Odlyha, N. S. Cohen, G. M. Foster, R. H. West, *Thermochim. Acta.* **2000**, *365*, 53.
[41] A. Lluveras, S. Boularand, A. Andreotti, M. Vendrell-Saz, *Appl. Phys. A Mater. Sci. Process.* **2010**, *99*, 363.
[42] K. Castro, A. Sarmiento, I. Martínez-Arkarazo, J. M. Madariaga, L. A. Fernández, *Anal. Chem.* **2008**, *80*, 4103.
[43] A. Zoppi, C. Lofrumento, N. F. C. Mendes, E. M. Castellucci, *Anal. Bioanal. Chem.* **2009**, *397*, 841.
[44] M. Pérez-Alonso, K. Castro, J. M. Madariaga, *Anal. Chim. Acta* **2006**, *571*, 121.
[45] A. M. Correia, M. J. V. Oliveira, R. J. H. Clark, M. I. Ribeiro, M. L. Duarte, *Anal. Chem.*, **2008**, *80*, 1482.
[46] I. Osticioli, N. F. C. Mendes, A. Nevin, F. P. S. C. Gil, M. Becucci, E. Castellucci, *Spectrochim. Acta Mol. Biomol. Spectros.* **2009**, *73*, 525.
[47] L. Robinet, M. Spring, S. Pagès-Camagna, *Anal. Methods.* **2013**, *5*, 4628.
[48] L. Samain, B. Gilbert, F. Grandjean, G. J. Long, D. Strivay, *J. Anal. At. Spectrom.* **2013**, *28*, 524.
[49] M.-J. Benquerença, N. F. C. Mendes, E. Castellucci, V. M. F. Gaspar, F. P. S. C. Gil, *J. Raman Spectrosc.* **2009**, *40*, 2135.
[50] P. Ferrer, S. Ruiz-Moreno, A. López-Gil, M. C. Chillón, C. Sandalinas, *J. Raman Spectrosc.* **2012**, *43*, 1805.
[51] R. J. H. Clark, L. Cridland, B. M. Kariuki, K. D. M. Harris, R. Withnall, *J. Chem. Soc. Dalton Trans.* **1995**, *16*, 2577.
[52] C. Miguel, A. Claro, A. P. Gonçalves, V. S. F. Muralha, M. J. Melo, *J. Raman Spectrosc.* **2009**, *40*, 1966.
[53] T. D. Chaplin, R. J. H. Clark, D. A. Scott, *J. Raman Spectrosc.* **2006**, *37*, 223.
[54] R. J. H. Clark, L. Curri, G. S. Henshaw, C. Laganara, *J. Raman Spectrosc.* **1997**, *28*, 105.
[55] F. Casadio, M. Leona, J. R. Lombardi, R. Van Duyne, *Acc. Chem. Res.* **2010**, *43*, 782.
[56] J. Thomas, J. H. Townsend, S. Hackney, M. Strlič, *Polym. Degrad. Stabil.* **2010**, *95*, 2343.
[57] A. Roy (Ed.), *Artists' Pigments: A Handbook of Their History and Characteristics*, Oxford University Press, New York, **1993**.
[58] H. G. M. Edwards, *Spectroscopy.* **2002**, *17*, 16.
[59] M. Pérez-Alonso, K. Castro, I. Martínez-Arkarazo, M. Angulo, M. A. Olazabal, J. M. Madariaga, *Anal. Bioanal. Chem.* **2004**, *379*, 42.
[60] H. G. M. Edwards, E. M. Newton, J. J. Russ, *J. Mol. Struct.* **2000**, *245*, 550.
[61] E. Mattei, G. de Vivo, A. De Santis, C. Gaetani, C. Pelosi, U. Santamaria, *J. Raman Spectrosc.* **2008**, *39*, 302.
[62] K. Wehlte, *The Materials and Techniques of Painting*, Kremer Pigments Incorporated, Aichstetten, New York, **1975**.
[63] R. Hudoklin, *Tehnologije materialov, ki se uporabljajo v slikarstvu*, Vzajemnost, Ljubljana, **1958**.
[64] R. L. Frost, W. N. Martens, L. Rintoul, E. Mahmutagic, J. T. Kloprogge, *J. Raman Spectrosc.* **2002**, *33*, 252.
[65] L. Debbichi, M. C. Marco de Lucas, J. F. Pierson, P. Krüger, *J. Phys. Chem. C* **2012**, *116*, 10232.